

AD-A182 324

APPLICATION OF GRASP (GENERAL ROTORCRAFT AEROMECHANICAL  
STABILITY PROGRAM. (U) NATIONAL AERONAUTICS AND SPACE  
ADMINISTRATION HOFFMANN FIELD C. H E HINNANT ET AL.

1/1

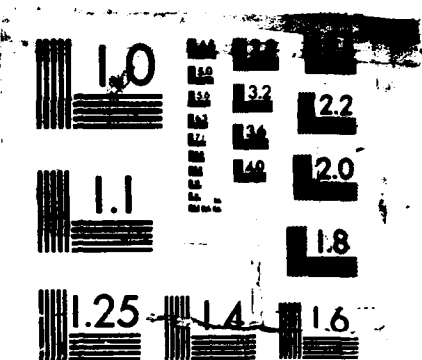
UNCLASSIFIED

APR 87

F/G 1/1

NL





MICROCOPY RESOLUTION TEST CHART

**AIAA'87**

DTIC FILE COPY

(1)

**AIAA-87-0953-CP**

**AD-A182 324**

**APPLICATION OF GRASP TO NONLINEAR  
ANALYSIS OF A CANTILEVER BEAM**

**Howard E. Hinnant**  
**U.S. Army Aviation Research and Technology Activity (AVSCOM)**  
**Ames Research Center**  
**Moffett Field, California**

**Dewey H. Hodges**  
**Georgia Institute of Technology**  
**Atlanta, Georgia**

This document has been approved  
for public release and sale; its  
distribution is unlimited.

STIC  
ELECTRICAL  
JUL 01 1987  
F A D

**AIAA Dynamics Specialists Conference**  
**April 9-10, 1987/Monterey, California**

**87**

**6 00 203**

# APPLICATION OF GRASP TO NONLINEAR ANALYSIS OF A CANTILEVER BEAM

Howard E. Hinnant\*

U. S. Army Aviation Research and Technology Activity (AVSCOM)  
Ames Research Center, Moffett Field, California

and

Dewey H. Hodges†  
Georgia Institute of Technology, Atlanta, Georgia

## Abstract

The General Rotorcraft Aeromechanical Stability Program (GRASP) was developed to analyse the steady-state and linearized dynamic behavior of rotorcraft in hovering and axial flight conditions. Because of the nature of problems GRASP was created to solve, the geometrically nonlinear behavior of beams is one area in which the program must perform well in order to be of any value. Numerical results obtained from GRASP are compared to both static and dynamic experimental data obtained for a cantilever beam undergoing large displacements and rotations caused by deformation. The correlation is excellent in all cases.

## Nomenclature

$b_1^P$	= basis vectors at the deformed beam tip
$b_1^R$	= basis vectors at the beam root
$c$	= beam width
$C_{ij}$	= direction cosine matrix relating the beam root and tip
$\epsilon$	= error in beam cross-sectional measurement
$E$	= modulus of elasticity
$I_2$	= geometrical cross-sectional property
$I_4$	= geometrical cross-sectional property
$p$	= projection of $b_1^P$ onto the $b_1^R - b_2^R$ plane
$t$	= beam thickness
$U$	= strain energy
$\alpha$	= material nonlinearity coefficient
$\beta$	= torsional deflection which was experimentally measured
$\kappa$	= curvature of the beam
$\phi_i$	= Rodrigues parameters
$\theta$	= load angle

## Introduction

The General Rotorcraft Aeromechanical Stability Program (GRASP)<sup>1</sup> is capable of treating the nonlinear static and linearized dynamic behavior of structures represented by collections of rigid-body and beam elements that may be connected in an arbitrary fashion and are permitted to have large relative motions. GRASP was developed primarily for analysis of the steady-state and linearized dynamic

This paper is declared a work of the U. S. Government and is not subject to copyright protection in the United States.

\* Aerospace Engineer, Rotorcraft Dynamics Division, Aeroflightdynamics Directorate. Member AIAA.

† Professor, School of Aerospace Engineering.  
Associate Fellow, AIAA.

behavior of rotorcraft in the hovering and axial flow flight conditions.

GRASP combines multibody and finite-element technology by taking the strong points from each area and integrated them together into a single, comprehensive package. GRASP differs from standard multibody programs by considering flexible-body and aeroelastic effects, including simple, nonlinear, unsteady aerodynamics. GRASP differs from standard finite-element programs by allowing multiple levels of substructures in which the substructures can move and/or rotate relative to others with no small-angle approximations. This capability facilitates the modeling of rotorcraft structures, including the rotating/nonrotating interface, and details of the blade/root kinematics for various rotor types. An overview of the features of GRASP as a program can be found in Ref. 1, while details of the analysis are given in Ref. 2. The theoretical basis of the analysis are addressed in companion papers.<sup>3,4</sup>

Because of the nature of the problems GRASP was created to solve, the geometrically nonlinear behavior of beams is one area in which the program must perform well in order to be of value. The main structural element in GRASP is the aeroelastic beam, a geometrically nonlinear beam element based on the kinematics, internal and inertial forces of Ref. 5 and the aerodynamics of Ref. 2. The element kinematics are valid for small strains and large rotations, but shear strains are neglected. The beam element degrees of freedom include (as generalized coordinates), rigid-body translations and rotations that are associated with the standard cubic and linear shape functions. These account for the usual twelve degrees of freedom found in beam finite-element analyses. In GRASP, however, an arbitrary number of additional generalized coordinates associated with higher-order polynomials<sup>6</sup> are also included, allowing the element to have a number of degrees of freedom that is arbitrarily more than the usual twelve, following the so-called "p-version" of the finite element method.<sup>7,8</sup>

This paper is to present numerical results from GRASP for comparison with static and dynamic experimental data for large deflections of an end-loaded cantilevered beam. (The experimental apparatus and procedures are only briefly described in this paper. Details of the experiment may be found in Ref. 9 and 10.) Determination of the beam properties for input into GRASP is described in detail. GRASP results are then presented along with results from previous analyses which are shown for comparison. While the present results do not exercise many of the features and power of GRASP, they do serve to validate much of the code dealing with the beam element's ability to model highly nonlinear behavior.

## Experiment

An experiment done at Princeton University<sup>9,10</sup> (under Aeroflightdynamics Directorate sponsorship), was selected as a test case with which to validate GRASP. This experiment consisted of measuring the static deformation and fundamental flatwise and edgewise natural frequencies of a uniform, nonrotating, cantilever beam with a mass attached to the tip (Fig. 1). The beam was slender and sufficiently flexible to undergo large displacements (still at small strains) due to the presence of the tip mass. Beam load angle and mass of the tip weight were varied throughout appropriate ranges.

The beam was instrumented with strain gages mounted at the root in the proper orientation to measure flatwise and edgewise natural frequencies. The end of the beam was securely mounted in a precision indexing chuck that provided a stable mount and accurate, repeatable angular settings. The static vertical and horizontal measurements were made with a caliper scale, measuring from a flat table with a reference grid affixed. The static torsional measurements were made with the aid of lightweight reference rods attached along the length of the beam and perpendicular to it. (See Ref. 10 for complete details.)

The beam was fabricated from 7075 aluminum. The mass density was assumed to be  $2.626 \times 10^{-4}$  lb.-sec.<sup>2</sup>/in.<sup>4</sup>. The length of the beam was measured to be 19.985 in. The thickness and width of the beam were measured at 0.1251 in. and 0.4999 in., respectively. Assuming a gravitational constant equal to 386.089 in./sec.<sup>2</sup>, the mass per unit length was determined to be  $1.6424 \times 10^{-8}$  lb.-sec.<sup>2</sup>/in.<sup>2</sup>. The mass moments of inertia were  $2.1420 \times 10^{-8}$  lb.-sec.<sup>2</sup> (flatwise) and  $3.4204 \times 10^{-7}$  lb.-sec.<sup>2</sup> (edgewise).

Determination of the appropriate values of bending stiffness proved to be more difficult. Both static and dynamic predicted behavior are sensitive to the value of the stiffnesses, therefore stiffnesses were determined as accurately as possible. Attempted inference of equivalent beam properties from classical linear formulas for deflection vs load for the two uncoupled cases, load angles of 0 and 90°, yields contradictory information — even when only small deflections are considered. At a load angle of 0° (the edgewise-bending case), linear theory is too stiff. But, at a load angle of 90° (the flatwise-bending case), linear theory is too soft. Similar contradictory information results when attempting to correlate natural frequencies of the unloaded beam according to linear-beam theory with experiment. This suggests that there is no one value of  $E$  that will yield accurate flatwise and edgewise bending stiffnesses if the measured cross-section dimensions are taken as exact and the theory is assumed to be linear. With the failure of linear theory, we turned to a simple, nonlinear, planar elastica model.<sup>11</sup> Even then, a standard value of the modulus of elasticity and measured cross-sectional dimensions in a standard elastica model, only fair agreement is obtained with planar, experimental, static deflections.

With the aforementioned problems in mind, a more innovative approach was called for. First, it was determined that only static data should be used because of supposed accuracy. Second, because transverse deflections for the uncoupled, no-tip-mass cases were recorded to be zero (even

though non-zero deflections should have been measurable), it was necessary to assume that the experimental data have deflections for the no-tip-mass case subtracted out. This latter point is not explicitly stated in Ref. 9 or 10, but from the present investigation, appears to be true. Finally, to allow for other effects not present in the simple elastica model, an extra parameter in the form of a material nonlinearity coefficient  $\alpha$ , was introduced. With the assumption that the beam is inextensible, the strain energy is expressed as

$$U = \frac{E}{2} (I_2 \kappa^2 + \frac{\alpha I_4 \kappa^4}{2}) \quad (1)$$

where  $\kappa$  is the curvature of the beam.  $I_2$  and  $I_4$  are geometrical cross-sectional properties defined as follows. For edgewise deflection:

$$\begin{aligned} I_2 &= \frac{c^3 t}{12} \\ I_4 &= \frac{c^5 t}{80} \end{aligned} \quad (2)$$

and for flatwise deflection:

$$\begin{aligned} I_2 &= \frac{ct^3}{12} \\ I_4 &= \frac{ct^5}{80} \end{aligned} \quad (3)$$

where  $c$  and  $t$  are the height and thickness dimensions, respectively, of the cross-section of the beam. Considering only the uncoupled, static deflections (load angles of 0 and 90°), an equation for the deflection of the tip of the beam was derived as a function of the beam bending stiffness and other unknowns. Once the equation for the tip deflection was derived, then a nonlinear least squares method was used to determine the best  $E I_2$  and  $\alpha$  that fit the experimental data for both uncoupled flatwise and uncoupled edgewise deflections. The value obtained for  $\alpha$  was ignored since GRASP does not consider material nonlinearity. The two values of  $E$  inferred from the bending stiffnesses and the cross-section geometry were averaged and multiplied by the cross-sectional area to obtain the axial stiffness. A value of Poisson's ratio equal to 0.31 was assumed and the shear modulus,  $G$ , was inferred from  $E$ . The following stiffnesses resulted:

$$\begin{aligned} \text{axial stiffness} &= 6.2856 \times 10^8 \text{ lb} \\ \text{flatwise stiffness} &= 8.4487 \times 10^2 \text{ lb-in}^2 \\ \text{edgewise stiffness} &= 1.2689 \times 10^4 \text{ lb-in}^2 \\ \text{torsional stiffness} &= 1.0538 \times 10^3 \text{ lb-in}^2 \end{aligned}$$

The ratio of the edgewise stiffness to the flatwise stiffness should be

$$\frac{c^2}{t^2} = 15.97 \quad (4)$$

However, this ratio, based on the above stiffnesses reported above, turned out to be

$$\frac{126.89}{8.4487} = 15.02 \quad (5)$$

If one assumes that this discrepancy is due to variations in width and thickness along the length of the beam, then the next question is how much variation would it take to cause this discrepancy? Assuming an error  $e$  in each measurement, and substituting in the measured values for  $c$  and  $t$ , one obtains the ratio as

$$\frac{(0.4999 + e)^2}{(0.1251 + e)^2} = 15.02 \quad (6)$$

yielding  $e = 0.0052$  in., a fairly small error. Thus, the inferred bending stiffnesses are not unreasonable.

The moments of inertia of the various tip masses used were estimated with some gross assumptions since these values are relatively unimportant. The only properties of the tip masses stated in Ref. 9 and 10 were the masses. There was also a photograph depicting a tip mass with a hollow cylindrical shape. With this information in mind, several assumptions were made: the density of the tip mass was that of steel (0.284 lb/in.<sup>3</sup>), the inner radius was 0.375 in., and finally, the length of the tip mass was equal to its outer diameter. With these assumptions, the moments of inertia for tip masses of varying size were calculated, (Table 1).

### GRASP Model

The GRASP model for the Princeton experiment is depicted in Fig. 2. Subsystem PRNCTN, the *model-type* subsystem generated internally by GRASP, represents the complete structure. The first explicitly defined subsystem is CANTBEAM. The frame of reference is defined to be coincident with the model frame except for a rotation about the  $x_3$  axis which is interpreted as the beam load angle. The subsystem contains two *structural nodes* named ROOT and TIP. ROOT is coincident with the CANTBEAM subsystem frame of reference, and has all of its degrees of freedom prescribed to zero (cantilever beam boundary conditions). TIP is defined to be located 19.985 in. from the frame along the  $x_3$  axis.

The first child of CANTBEAM is an *aeroelastic beam element* named BEAM. An *aeroelastic beam connectivity* constraint associates the element's root and tip nodes with the nodes ROOT and TIP in the subsystem CANTBEAM. The definition of the element includes specifying the orders of the polynomials used to represent the displacements. The typical approach in finite element programs would be to use several elements with the transverse displacements approximated by cubic polynomials, and the axial displacement and torsion approximated by linear polynomials. Instead, for this analysis we use one element with eighth-order polynomials for bending and sixth-order polynomials for axial displacement and torsion. This yields a total of 32 element degrees of freedom (6 of which are constrained out by the clamped-end condition). Essentially the same results are obtained when the order of each polynomial is reduced by one.

Subsystem WEIGHT, the second child of CANTBEAM, is a *rigid-body mass element* that is defined to be co-

incident with the node TIP. Its definition specifies the mass and the mass moments of inertias about all three principal axes.

### Correlation of GRASP Results With Experiment

GRASP expresses static rotations in terms of Rodrigues parameters,<sup>12,2</sup> so a minor amount of postprocessing is needed to convert the GRASP output to the projected angle, ( $\beta$ ), as measured in Ref. 9, (Fig. 3). Consider the orthogonal triad at the root of the beam that remains aligned with the principal axes at the root. Introduce a dextral triad of unit vectors associated with those axes denoted by  $b_i^R$  for  $i = 1, 2$ , and 3. Now consider a similar dextral triad at the tip of the beam, denoted by  $b_i^P$  for  $i = 1, 2$ , and 3, where the deflections and rotations were measured in the experiments. The relationship between the triads is simply

$$b_i^P = C_{ij} b_j^R \quad (7)$$

where a repeated index implies summation. A line along the width of the cross-section is then aligned with  $b_1^P = C_{11} b_1^R$ . Now consider the projection of  $b_1^P$  in the plane determined by  $b_1^R$  and  $b_2^R$  denoted by  $p$ . The expression for  $p$  can be easily determined as

$$\begin{aligned} p &= b_1^P - b_1^P \cdot b_3^R b_3^R \\ &= C_{11} b_1^R + C_{12} b_2^R \end{aligned} \quad (8)$$

The angle measured in the experiments is the angle between  $p$  and  $b_1^R$ . From Fig. 3, it is clear that

$$\beta = \sin^{-1} \frac{C_{12}}{\sqrt{1 - C_{13}^2}} \quad (9)$$

In terms of Rodrigues parameters\*

$$\begin{aligned} C_{12} &= \frac{\phi_3 + \frac{\phi_1 \phi_2}{2}}{1 + \frac{\phi_1^2 + \phi_2^2 + \phi_3^2}{4}} \\ C_{13} &= \frac{-\phi_2 + \frac{\phi_1 \phi_3}{2}}{1 + \frac{\phi_1^2 + \phi_2^2 + \phi_3^2}{4}} \end{aligned} \quad (10)$$

where  $\phi_1$ ,  $\phi_2$ , and  $\phi_3$  are the Rodrigues parameters associated with the rotation of the tip node.

Also, all GRASP deflections have the deflections for no tip mass subtracted out before the results are plotted with the experimental data. All frequencies calculated by GRASP were converted from rad/sec to Hz.

First, results are presented for a 1-lb. tip mass. Figure 4 shows the static deflections vs load angle. The GRASP correlation for flatwise and edgewise is excellent. Results from Ref. 13 and 14 are shown here for comparison, with results from Ref. 14 presented only for the torsional deflections. Transverse displacements from Ref. 14 were only

\* It should be noted that the matrix of direction cosines in this work is the transpose of the one in Ref. 12 and that the Rodrigues parameters used in GRASP differ from those of Ref. 12 by a factor of 2.

available for load angles of 30 and 40°, and therefore, a complete load angle sweep could not be shown. It should be noted, however, that the transverse displacement results did agree well both with experiment and with GRASP.

There were no dynamic results from Ref. 14. The calculations presented in Ref. 13 are based on the equations of Ref. 15. This analysis is restricted to moderate rotations caused by deformation, such that the squares of the rotational components are small compared to unity. Reference 13 is not as accurate throughout the entire range of load angle as GRASP. For torsional deflection, the GRASP calculations cut right through the middle of the experimental scatter. The experimental scatter here is so large, however, that it is impossible to say which curve best fits the data. Figure 5 displays the flatwise and edgewise frequencies vs load angle. The GRASP results are only slightly offset from the experimental values, and follow the trend exactly. The average error is approximately 0.5%. Reference 13 does not pick up the trend for the flatwise frequency, however it does follow the trend for the edgewise frequency. Reference 14 does not consider the dynamics.

The 2-lb. tip-mass results are presented next. Here the torsional data have much less scatter than in the 1-lb. case. Again, GRASP correlates excellently with the static deflection as shown in Fig. 6. Also again, Ref. 13 is close but tends to deviate through certain portions of the load angle sweep. This deviation from the data is large for load angles above 40°. Reference 14, however, correlates quite well with the static data. Figure 7 shows the flatwise and edgewise frequencies. The GRASP predictions are again slightly low for both of the frequencies, but follow the trends very nicely. Reference 13 while matching the data fairly well at 0° load angle, strays from the data at higher load angles.

Figure 8 presents the static results from the 3-lb. tip-mass case. All three analyses appear to match the data well over the range shown. However, Ref. 13 results are available for only a load angle up to 15°, while Ref. 14 calculated results up to 45°. The failure of Ref. 14 to converge past 15° is probably a result of the restriction to moderate rotation in that analysis. This is not a problem with GRASP, since GRASP has no such restriction. In Fig. 9 the flatwise and edgewise frequency sweeps are shown for the experimental data and the GRASP analysis. The correlation is excellent.

For the 4-lb. tip-mass case there was not a very large experimental sweep available because of the large displacements which the beam underwent. GRASP did, however, correlate very well in the statics, Fig. 10, and the dynamics, Fig. 11. Reference 14 also correlates well with the static torsional deflection data.

Figures 12 and 13 summarize flatwise and edgewise frequency vs tip mass. The lateral buckling load can be inferred from Fig. 12. As the tip mass increases, the flatwise frequency will tend toward zero. When lateral buckling is imminent, the frequency will drop to zero very rapidly as indicated by both GRASP and Ref. 13. The edgewise frequency shown in Fig. 13 does not reach zero since there is no buckling in this mode.

It should be noted that the analysis of Ref. 13 suffers from being restricted to moderate rotations. Reference 14 does much better than Ref. 13 in predicting the behavior of this configuration because equations used therein are specialized for the type of structure used in the experiment. The equations of Ref. 14 are essentially identical to those of Ref. 13 except that certain terms of third degree in the unknowns are added to the analysis based on the observation that the coefficients of those terms are large. The size of those coefficients is a function of the ratio of the stiffnesses (thus depending on the cross-section geometry). These added terms would not be appropriate if the cross-section geometry were such that the stiffnesses were of the same order of magnitude. It is important to note that the equations in the GRASP analysis do not require that terms be added or removed in this manner. This is an important consideration for general-purpose analyses, the equations for which should not have need of alteration merely because of changes in properties.

### Concluding Remarks

GRASP is a general-purpose program with both the detail and the generality to accurately model the end-loaded cantilever beam, as presented herein, as well or better than the special-purpose analyses in Ref. 13 and 14. Although this experiment demonstrated significant nonlinear behavior both statically and dynamically, GRASP accurately predicts the results. The equations upon which GRASP is based are not restricted as far as the magnitudes of displacement or rotation. Only the strains are required to be small compared to unity. The GRASP analysis is shown herein to be valid for these types of problems. As noted in the introduction, however, the present validation does not exercise many of the capabilities of the program. Also, as pointed out in Ref. 1, the analysis does need to be extended to treat beams for which shear deformation would be important.

### Acknowledgment

The second author was supported by grant E-16-697 from the Georgia Tech Research Center.

### References

<sup>1</sup>Hodges, D. H., Hopkins, A. S., Kuns, D. L., and Hinnant, H. E., "Introduction to GRASP - General Rotorcraft Aeromechanical Stability Program - A Modern Approach to Rotorcraft Modeling," Proceedings of the 42nd Annual Forum of the American Helicopter Society, Washington, D.C., June, 1986.

<sup>2</sup>Hodges, D. H., Hinnant, H. E., Hopkins, A. S., and Kuns, D. L., "General Rotorcraft Aeromechanical Stability Program (GRASP) Theoretical Manual," NASA TM in preparation, 1987.

<sup>3</sup>Hopkins, A. S., and Likins, P. W., "Analysis of Structures with Rotating, Flexible Substructures," Proceedings of the AIAA Dynamics Specialists Conference, Monterey, California, April, 1987.

<sup>6</sup>Hedges, D. H., Hopkins, A. S., and Kuns, D. L., "Analysis of Structures with Rotating, Flexible Substructures Applied to Rotorcraft Aeroelasticity in GRASH," Proceedings of the AIAA Dynamics Specialists Conference, Monterey, California, April, 1987.

<sup>7</sup>Hedges, D. H., "Nonlinear Equations for Dynamics of Pretwisted Beams Undergoing Small Strains and Large Rotations," NASA TP-2470, 1985.

<sup>8</sup>Hedges, D. H., "Orthogonal Polynomials as Variable-Order Finite Element Shape Functions," *AIAA Journal*, Vol. 21, No. 5, May 1983, pp. 796 - 797.

<sup>9</sup>Szabo, B. A., "Some Recent Developments in Finite Element Analysis," *Computers and Mathematics with Applications*, Vol. 5, 1979, pp. 99 - 115.

<sup>10</sup>Hedges, D. H., and Rutkowski, M. J., "Free-Vibration Analysis of Rotating Beams by a Variable-Order Finite Element Method," *AIAA Journal*, Vol. 19, No. 11, Nov. 1981, pp. 1459 - 1466.

<sup>11</sup>Dowell, E. H., and Traybar, J., "An Experimental Study of the Non-linear Stiffness of a Rotor Blade Undergoing Flap, Lag and Twist Deformations," AMS Report No. 1194, Princeton University, Jan. 1975.

<sup>12</sup>Dowell, E. H., and Traybar, J., "An Experimental Study of the Non-linear Stiffness of a Rotor Blade Undergoing Flap, Lag and Twist Deformations," AMS Report No. 1257, Princeton University, Dec. 1975.

<sup>13</sup>Love, A. E. H., *A Treatise on the Mathematical Theory of Elasticity*, Fourth Ed., Dover Publications, New York, 1944, pp. 381 - 426.

<sup>14</sup>Kane, T. R., Likins, P. W., and Levinson, D. A., *Space-craft Dynamics*, McGraw-Hill, New York, 1983, pp. 1 - 90.

<sup>15</sup>Dowell, E. H., Traybar, J., and Hedges, D. H., "An Experimental-Theoretical Correlation Study of Non-linear Bending and Torsion Deformations of a Cantilever Beam," *Journal of Sound and Vibration*, Vol. 50, No. 4, 1977, pp. 533 - 544.

<sup>16</sup>Rosen, A., and Friedmann, P., "The Nonlinear Behavior of Elastic Slender Straight Beams Undergoing Small Strains and Moderate Rotations," *Journal of Applied Mechanics*, Vol. 46, March 1979, pp. 161 - 168.

<sup>17</sup>Hedges, D. H., and Dowell, E. H., "Nonlinear Equations of Motion for the Elastic Bending and Torsion of Twisted Nonuniform Rotor Blades," NASA TN D-7818, 1974.

Table 1 Estimated Inertial Properties of Tip Mass

Weight (lb.)	Lateral Moments of Inertia (lb.-in.-sec. <sup>2</sup> )	Axial Moment of Inertia (lb.-in.-sec. <sup>2</sup> )
1.0	$1.0822 \times 10^{-3}$	$8.2356 \times 10^{-4}$
2.0	$3.3676 \times 10^{-3}$	$2.6784 \times 10^{-3}$
3.0	$6.5673 \times 10^{-3}$	$5.3169 \times 10^{-3}$
4.0	$1.0561 \times 10^{-2}$	$8.6363 \times 10^{-3}$
5.0	$1.5276 \times 10^{-2}$	$1.2573 \times 10^{-2}$
6.0	$2.0658 \times 10^{-2}$	$1.7083 \times 10^{-2}$
7.0	$2.6670 \times 10^{-2}$	$2.2131 \times 10^{-2}$
8.0	$3.3278 \times 10^{-2}$	$2.7691 \times 10^{-2}$
9.0	$4.0457 \times 10^{-2}$	$3.3741 \times 10^{-2}$
10.0	$4.8185 \times 10^{-2}$	$4.0261 \times 10^{-2}$
10.42	$5.1589 \times 10^{-2}$	$4.3135 \times 10^{-2}$
10.46	$5.1919 \times 10^{-2}$	$4.3413 \times 10^{-2}$



For

W.M.

1.0

1.1

1.2

1.3

1.4

1.5

1.6

1.7

1.8

1.9

1.10

1.11

1.12

1.13

1.14

1.15

1.16

1.17

1.18

1.19

1.20

1.21

1.22

1.23

1.24

1.25

1.26

1.27

1.28

1.29

1.30

1.31

1.32

1.33

1.34

1.35

1.36

1.37

1.38

1.39

1.40

1.41

1.42

1.43

1.44

1.45

1.46

1.47

1.48

1.49

1.50

1.51

1.52

1.53

1.54

1.55

1.56

1.57

1.58

1.59

1.60

1.61

1.62

1.63

1.64

1.65

1.66

1.67

1.68

1.69

1.70

1.71

1.72

1.73

1.74

1.75

1.76

1.77

1.78

1.79

1.80

1.81

1.82

1.83

1.84

1.85

1.86

1.87

1.88

1.89

1.90

1.91

1.92

1.93

1.94

1.95

1.96

1.97

1.98

1.99

1.00

1.01

1.02

1.03

1.04

1.05

1.06

1.07

1.08

1.09

1.10

1.11

1.12

1.13

1.14

1.15

1.16

1.17

1.18

1.19

1.20

1.21

1.22

1.23

1.24

1.25

1.26

1.27

1.28

1.29

1.30

1.31

1.32

1.33

1.34

1.35

1.36

1.37

1.38

1.39

1.40

1.41

1.42

1.43

1.44

1.45

1.46

1.47

1.48

1.49

1.50

1.51

1.52

1.53

1.54

1.55

1.56

1.57

1.58

1.59

1.60

1.61

1.62

1.63

1.64

1.65

1.66

1.67

1.68

1.69

1.70

1.71

1.72

1.73

1.74

1.75

1.76

1.77

1.78

1.79

1.80

1.81

1.82

1.83

1.84

1.85

1.86

1.87

1.88

1.89

1.90

1.91

1.92

1.93

1.94

1.95

1.96

1.97

1.98

1.99

1.00

1.01

1.02

1.03

1.04

1.05

1.06

1.07

1.08

1.09

1.10

1.11

1.12

1.13

1.14

1.15

1.16

1.17

1.18

1.19

1.20

1.21

1.22

1.23

1.24

1.25

1.26

1.27

1.28

1.29

1.30

1.31

1.32

1.33

1.34

1.35

1.36

1.37

1.38

1.39

1.40

1.41

1.42

1.43

1.44

1.45

1.46

1.47

1.48

1.49

1.50

1.51

1.52

1.53

1.54

1.55

1.56

1.57

1.58

1.59

1.60

1.61

1.62

1.63

1.64

1.65

1.66

1.67

1.68

1.69

1.70

1.71

1.72

1.73

1.74

1.75

1.76

1.77

1.78

1.79

1.80

1.81

1.82

1.83

1.84

1.85

1.86

1.87

1.88

1.89

1.90

1.91

1.92

1.93

1.94

1.95

1.96

1.97

1.98

1.99

1.00

1.01

1.02

1.03

1.04

1.05

1.06

1.07

1.08

1.09

1.10

1.11

1.12

1.13

1.14

1.15

1.16

1.17

1.18

1.19

1.20

1.21

1.22

1.23

1.24

1.25

1.26

1.27

1.28

1.29

1.30

1.31

1.32

1.33

1.34

1.35

1.36

1.37

1.38

1.39

1.40

1.41

1.42

1.43

1.44

1.45

1.46

1.47

1.48

1.49

1.50

1.51

1.52

1.53

1.54

1.55

1.56

1.57

1.58

1.59

1.60

1.61

1.62

1.63

1.64

1.65

1.66

1.67

1.68

1.69

1.70

1.71

1.72

1.73

1.74

1.75

1.76

1.77

1.78

1.79

1.80

1.81

1.82

1.83

1.84

1.85

1.86

1.87

1.88

1.89

1.90

1.91

1.92

1.93

1.94

1.95

1.96

1.97

1.98

1.99

1.00

1.01

1.02

1.03

1.04

1.05

1.06

1.07

1.08

1.09

1.10

1.11

1.12

1.13

1.14

1.15

1.16

1.17

1.18

1.19

1.20

1.21

1.22

1.23

1.24

1.25

1.26

1.27

1.28

1.29

1.30

1.31

1.32

1.33

1.34

1.35

1.36

1.37

1.38

1.39

1.40

1.41

1.42

1.43

1.44

1.45

1.46

1.47

1.48

1.49

1.50

1.51

1.52

1.53

1.54

1.55

1.56

1.57

1.58

1.59

1.60

1.61

1.62

1.63

1.64

1.65

1.66

1.67

1.68

1.69

1.70

1.71

1.72

1.73

1.74

1.75

1.76

1.77

1.78

1.79

1.80

1.81

1.82

1.83

1.84

1.85

1.86

1.87

1.88

1.89

1.90

1.91

1.92

1.93

1.94

1.95

1.96

1.97

1.98

1.99

1.00

1.01

1.02

1.03

1.04

1.05

1.06

1.07

1.08

1.09

1.10

1.11

1.12

1.13

1.14

1.15

1.16

1.17

1.18

1.19

1.20

1.21

1.22

1.23

1.24

1.25

1.26

1.27

1.28

1.29

1.30

1.31

1.32

1.33

1.34

1.35

1.36

1.37

1.38

1.39

1.40

1.41

1.42

1.43

1.44

1.45

1.46

1.47

1.48

1.49

1.50

1.51

1.52

1.53

1.54

1.55

1.56

1.57

1.58

1.59

1.60

1.61

1.62

1.63

1.64

1.65

1.66

1.67

1.68

1.69

1.70

1.71

1.72

1.73

1.74

1.75

1.76

1.77

1.78

1.79

1.80

1.81

1.82

1.83

1.84

1.85

1.86

1.87

1.88

1.89

1.90

1.91

1.92

1.93

1.94

1.95

1.96

1.97

1.98

1.99

1.00

1.01

1.02

1.03

1.04

1.05

1.06

1.07

1.08

1.09

1.10

1.11

1.12

1.13

1.14

1.15

1.16

1.17

1.18

1.19

1.20

1.21

1.22

1.23

1.24

1.25

1.26

1.27

1.28

1.29

1.30

1.31

1.32

1.33

1.34

1.35

1.36

1.37

1.38

1.39

1.40

1.41

1.42

1.43

1.44

1.45

1.46

1.47

1.48

1.49

1.50

1.51

1.52

1.53

1.54

1.55

1.56

1.57

1.58

1.59

1.60

1.61

1.62

1.63

1.64

1.65

1.66

1.67

1.68

1.69

1.70

1.71

1.72

1.73

1.74

1.75

1.76

1.77

1.78

1.79

1.80

1.81

1.82

1.83

1.84

1.85

1.86

1.87

1.88

1.89

1.90

1.91

1.92

1.93

1.94

1.95

1.96

1.97

1.98

1.99

1.00

1.01

1.02

1.03

1.04

1.05

1.06

1.07

1.08

1.09

1.10

1.11

1.12

1.13

1.14

1.15

1.16

1.17

1.18

1.19

1.20

1.21

1.22

1.23

1.24

1.25

1.26

1.27

1.28

1.29

1.30

1.31

1.32

1.33

1.34

1.35

1.36

1.37

1.38

1.39

1.40

1.41

1.42

1.43

1.44

1.45

1.46

1.47

1.48

1.49

1.50

1.51

1.52

1.53

1.54

1.55

1.56

1.57

1.58

1.59

1.60

1.61

1.62

1.63

1.64

1.65

1.66

1.67

1.68

1.69

1.70

1.71

1.72

1.73

1.74

1.75

1.76

1.77

1.78

1.79

1.80

1.81

1.82

1.83

1.84

1.85

1.86

1.87

1.88

1.89

1.90

1.91

1.92

1.93

1.94

1.95

1.96

1.97

1.98

1.99

1.00

1.01

1.02

1.03

1.04

1.05

1.06

1.07

1.08

1.09

1.10

1.11

1.12

1.13

1.14

1.15

1.16

1.17

1.18

1.19

1.20

1.21

1.22

1.23

1.24

1.25

1.26

1.27

1.28

1.29

1.30

1.31

1.32

1.33

1.34

1.35

1.36

1.37

1.38

1.39

1.40

1.41

1.42

1.43

1.44

1.45

1.46

1.47

1.48

1.49

1.50

1.51

1.52

1.53

1.54

1.55

1.56

1.57

1.58

1.59

1.60

1.61

1.62

1.63

1.64

1.65

1.66

1.67

1.68

1.69

1.70

1.71

1.72

1.73

1.74

1.75

1.76

1.77

1.78

1.79

1.80

1.81

1.82

1.83

1.84

1.85

1.86

1.87

1.88

1.89

1.90

1.91

1.92

1.93

1.94

1.95

1.96

1.97

1.98

1.99

1.00

1.01

1.02

1.03

1.04

1.05

1.06

1.07

1.08

1.09

1.10

1.11

1.12

1.13

1.14

1.15

1.16

1.17

1.18

1.19

1.20

1.21

1.22

1.23

1.24

1.25

1.26

1.27

1.28

1.29

1.30

1.31

1.32

1.33

1.34

1.35

1.36

1.37

1.38

1.39

1.40

1.41

1.42

1.43

1.44

1.45

1.46

1.47

1.48

1.49

1.50

1.51

1.52

1.53

1.54

1.55

1.56

1.57

1.58

1.59

1.60

1.61

1.62

1.63

1.64

1.65

1.66

1.67

1.68

1.69

1.70

1.71

1.72

1.73

1.74

1.75

1.76

1.77

1.78

1.79

1.80

1.81

1.82

1.83

1.84

1.85

1.86

1.87

1.88

1.89

1.90

1.91

1.92

1.93

1.94

1.95

1.96

1.97

1.98

1.99

1.00

1.01

1.02

1.03</

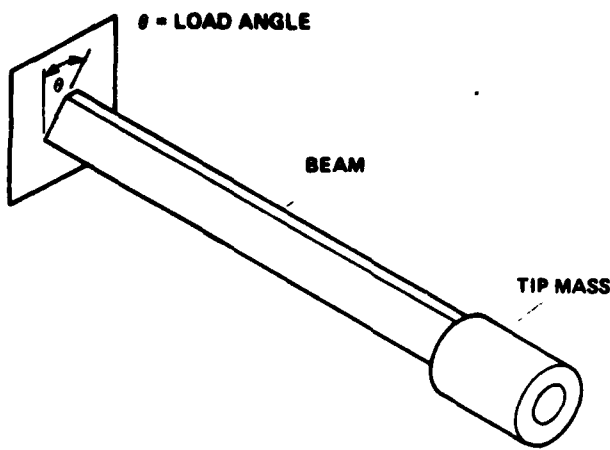


Fig. 1 Schematic of the Princeton beam experimental apparatus.

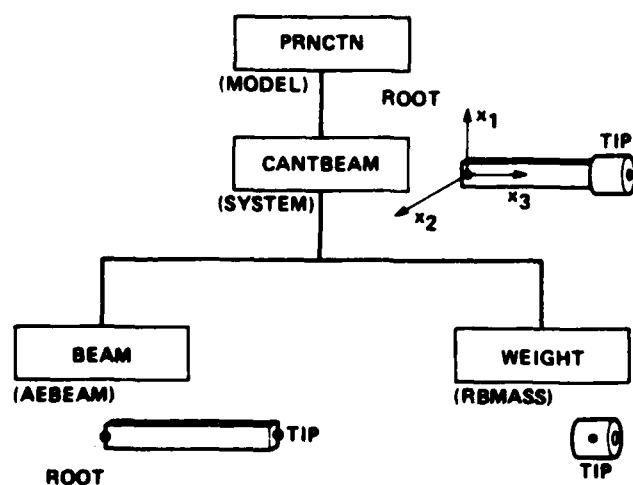


Fig. 2 Hierarchical GRASP model of the Princeton beam.

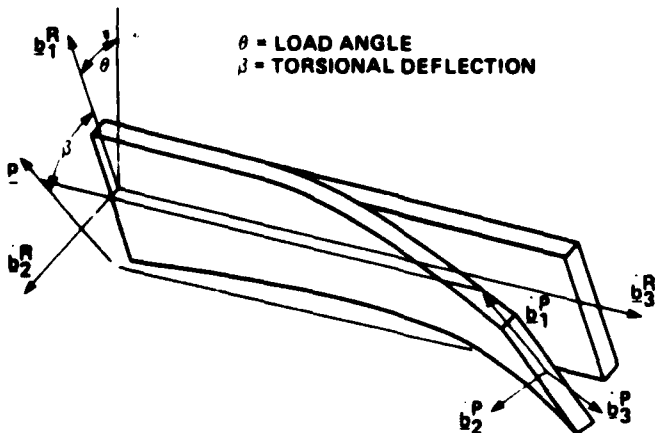


Fig. 3 Schematic of undeformed and deformed beams showing  $b_i^R$  (along the fixed axes at the root),  $b_i^P$  (along the principal axes at the tip),  $p$  (the projection of  $b_i^P$  onto the plane determined by  $b_1^R$  and  $b_2^R$ ), and  $\beta$  (the angle measured in the experiment).

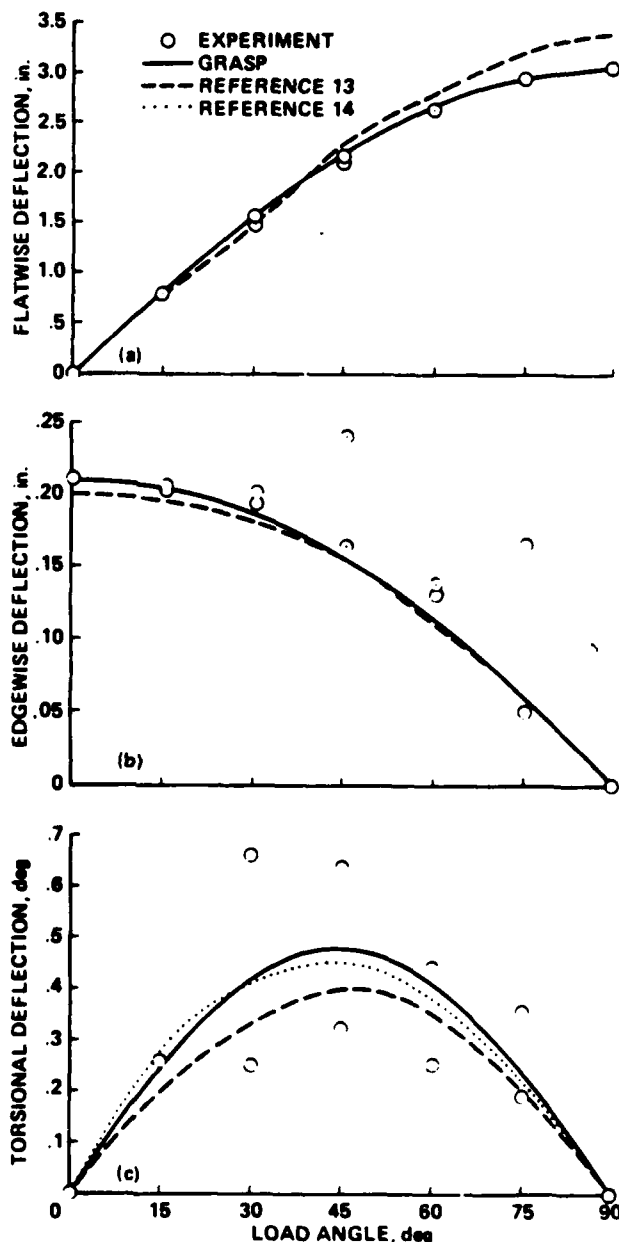


Fig. 4 GRASP correlation with the Princeton experiment (1-lb. tip mass): static deflections.

a) flatwise vs load angle.

b) edgewise vs load angle.

c) torsional vs load angle.

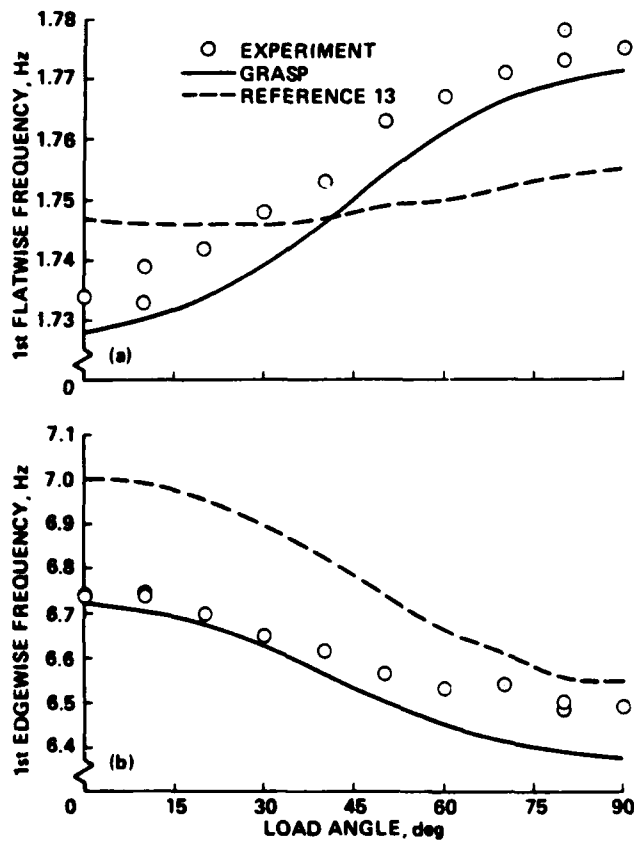


Fig. 5 GRASP correlation with the Princeton experiment (1-lb. tip mass): first flatwise and first edgewise frequencies vs load angle.

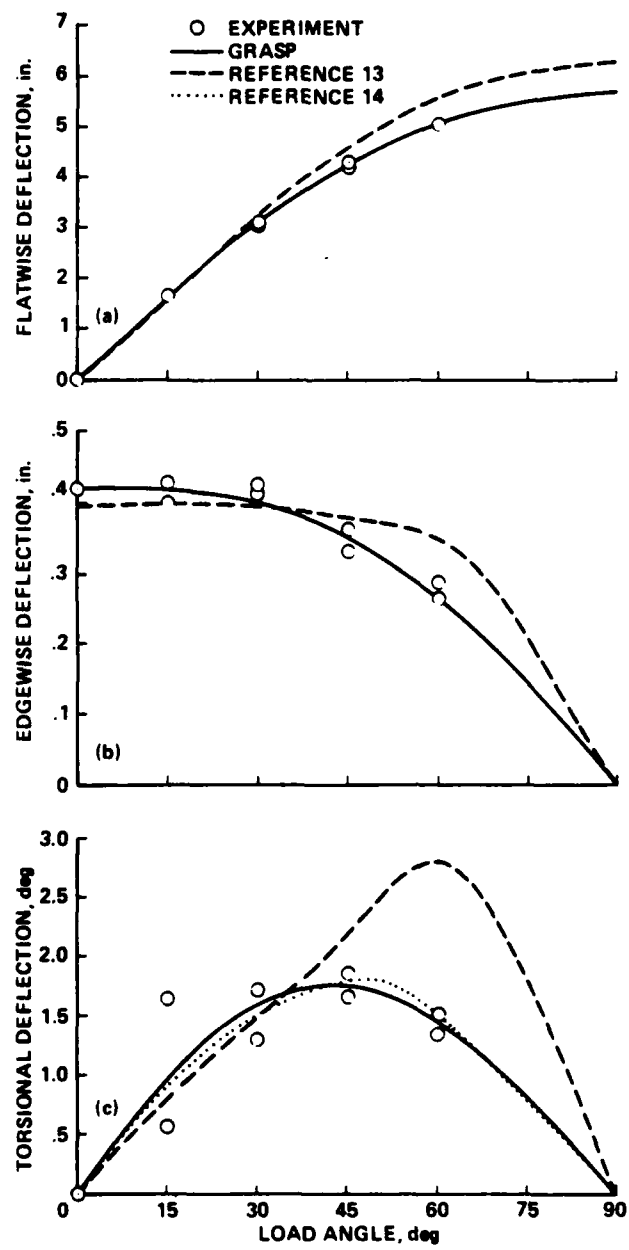


Fig. 6 GRASP correlation with the Princeton experiment (2-lb. tip mass): static deflections.

- flatwise vs load angle.
- edgewise vs load angle.
- torsional vs load angle.

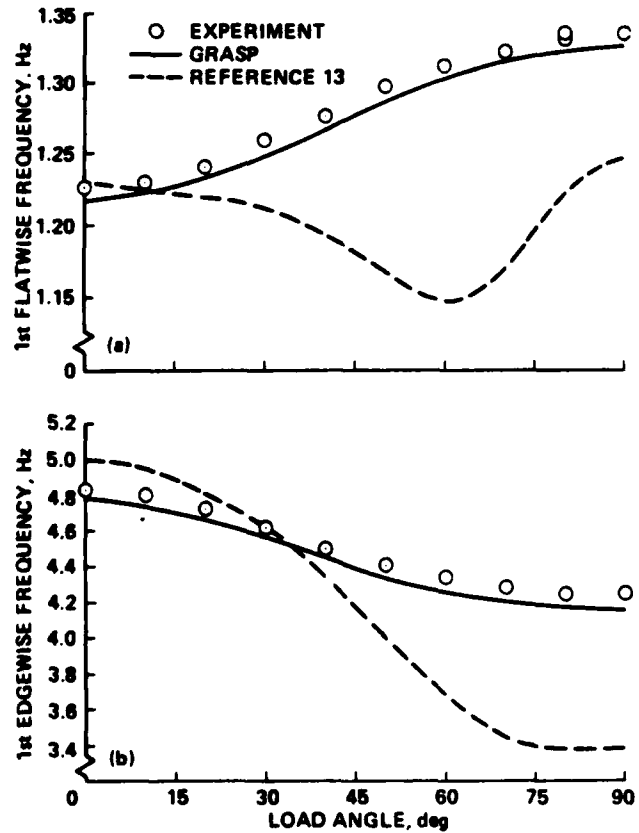


Fig. 7 GRASP correlation with the Princeton experiment (2-lb. tip mass): first flatwise and first edgewise frequencies vs load angle.

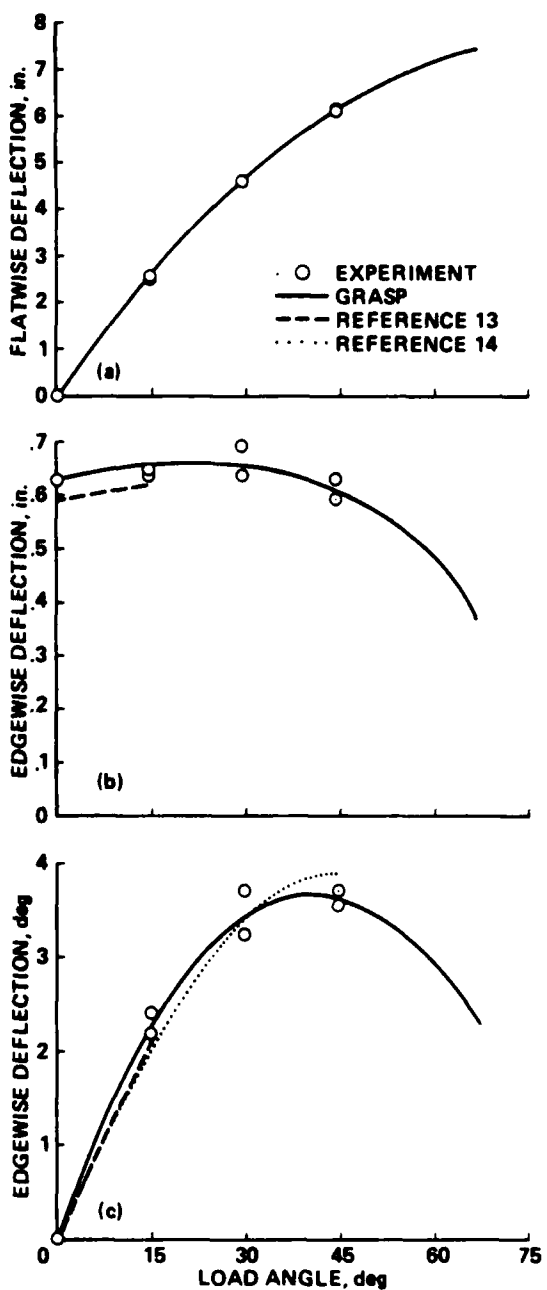


Fig. 8 GRASP correlation with the Princeton experiment (3-lb. tip mass): static deflections.  
 a) flatwise vs load angle.  
 b) edgewise vs load angle.  
 c) torsional vs load angle.

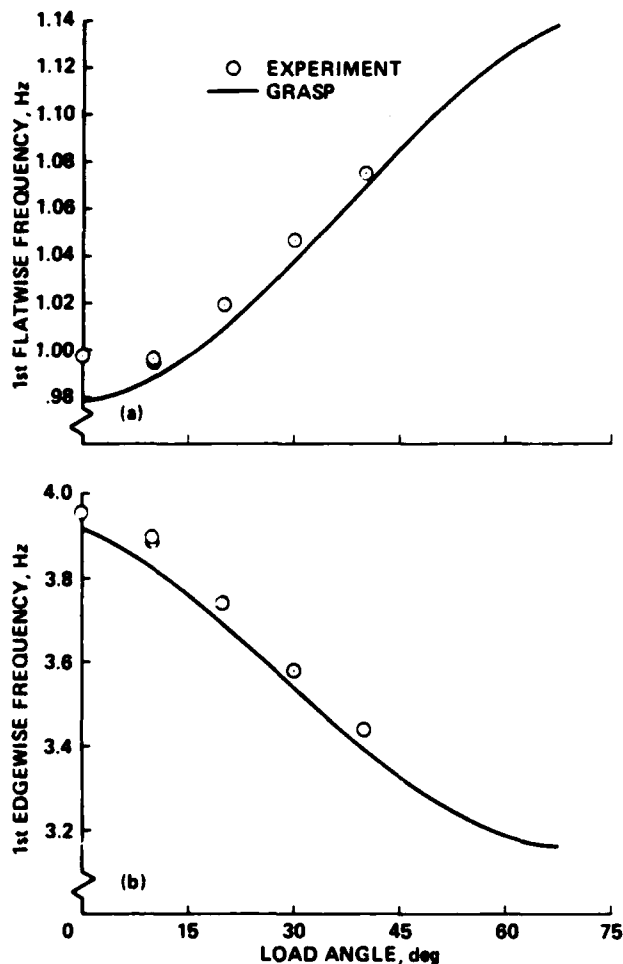


Fig. 9 GRASP correlation with the Princeton experiment (3-lb. tip mass): first flatwise and first edgewise frequencies vs load angle.

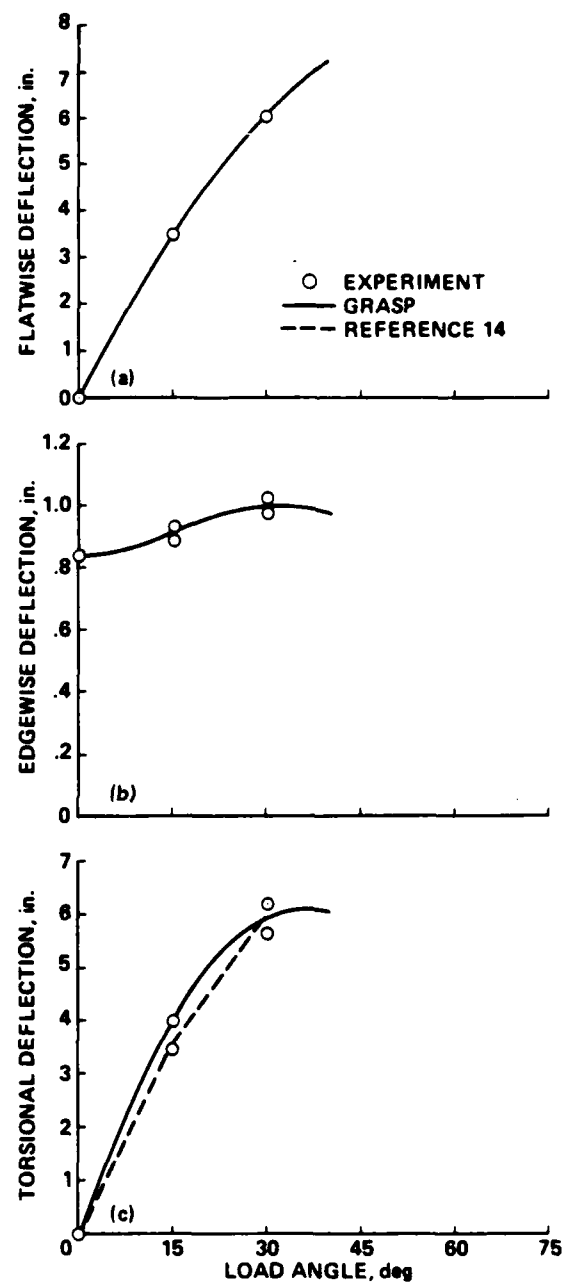


Fig. 10 GRASP correlation with the Princeton experiment (4-lb. tip mass): static deflections.

- a) flatwise vs load angle.
- b) edgewise vs load angle.
- c) torsional vs load angle.

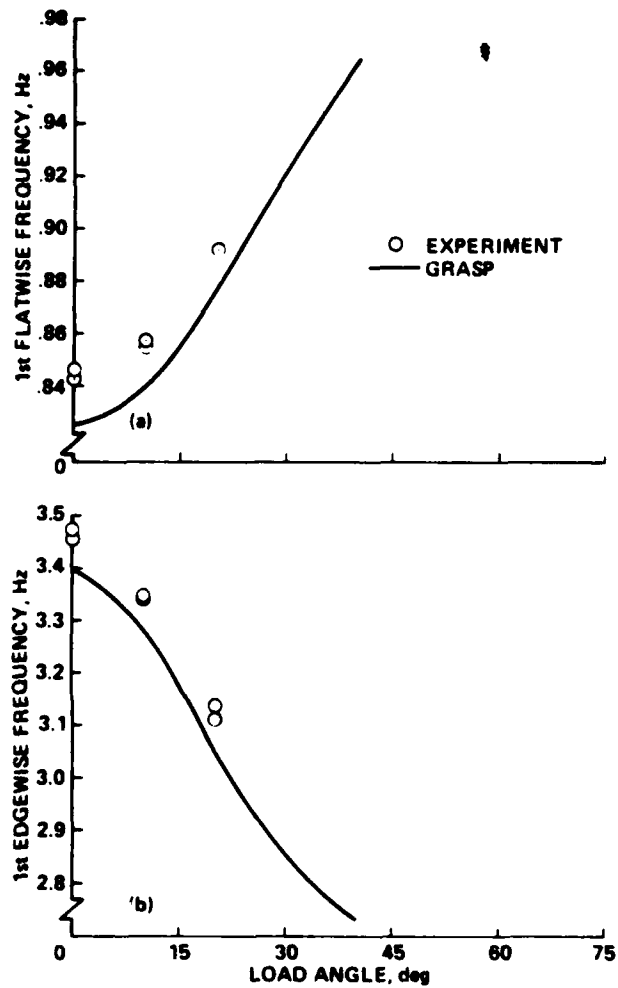


Fig. 11 GRASP correlation with the Princeton experiment (4-lb. tip mass): first flatwise and first edgewise frequencies vs load angle.

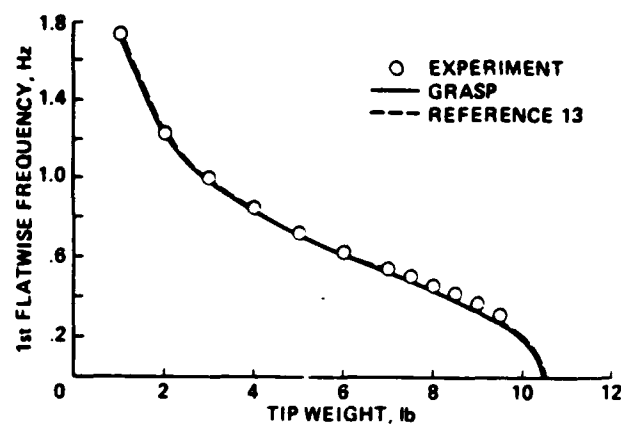


Fig. 12 GRASP correlation with the Princeton experiment: first flatwise frequency vs weight of tip mass.

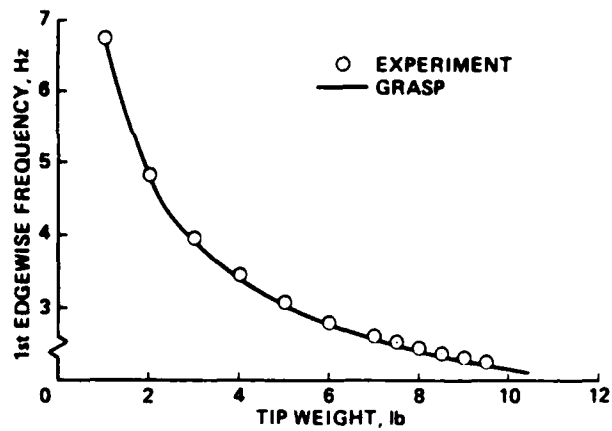


Fig. 13 GRASP correlation with the Princeton experiment: first edgewise frequency vs weight of tip mass.

E

N

D

S

S

Ptic